

# Talking Face Generation by Conditional Recurrent Adversarial Network

Yang Song<sup>\*1</sup>, Jingwen Zhu<sup>\*2</sup>, Xiaolong Wang<sup>2</sup>, and Hairong Qi<sup>1</sup>

<sup>1</sup> The University of Tennessee, Knoxville

<sup>2</sup> Samsung Research America

{ysong18,hqi}@utk.edu, {visionxiaolong,zhujingwen8942}@gmail.com

**Abstract.** Given an arbitrary face image and an arbitrary speech clip, the proposed work attempts to generating the talking face video with accurate lip synchronization while maintaining smooth transition of both lip and facial movement over the entire video clip. Existing works either do not consider temporal dependency on face images across different video frames thus easily yielding noticeable/abrupt facial and lip movement or are only limited to the generation of talking face video for a specific person thus lacking generalization capacity. We propose a novel conditional video generation network where the audio input is treated as a condition for the recurrent adversarial network such that temporal dependency is incorporated to realize smooth transition for the lip and facial movement. In addition, we deploy a multi-task adversarial training scheme in the context of video generation to improve both photo-realism and the accuracy for lip synchronization. Finally, based on the phoneme distribution information extracted from the audio clip, we develop a sample selection method that effectively reduces the size of the training dataset without sacrificing the quality of the generated video. Extensive experiments on both controlled and uncontrolled datasets demonstrate the superiority of the proposed approach in terms of visual quality, lip sync accuracy, and smooth transition of lip and facial movement, as compared to the state-of-the-art.

**Keywords:** Video Generation, Adversarial Training, Recurrent Generation Network

## 1 Introduction

Speech audio to video generation aims to generate naturally looking talking face synchronized with the given input audio. Aside from being an interesting topic from a research standpoint, it has a wide-range of applications, including, for example, video bandwidth reduction [1], face animation, and other entertainment applications. The challenge of the talking face generation problem is three-fold. First, video generation is, in general, more challenging than still image generation since humans are sensitive with any subtle artifacts and temporal discontinuities.

---

\* indicates the authors contribute equally

Second, audio to video speech generation poses extra rigid requirement on the accuracy of lip synchronization. Third, due to the large variation in human pose, talking speed and style, how to train a model with the generalization capacity for both unseen audio and face image is quite challenging.

Video generation is intrinsically a temporal-dependent problem. However, most existing works tend to formulate it as a temporal-independent image generation problem, where the entire audio clip is usually cropped into audio segments by a sliding window and each video frame is generated independently only based on the individual audio segment. For example, one closely related work proposed by Chung et al. [2] directly embeds the encoded visual (containing the identity information) and audio feature (reflecting the lip movement condition) as the input fed into the decoder network to generate face image frame. The final video is generated by stacking all frames together where each frame is independently treated. Similarly, Karras et al. [3] uses a sliding window to extract audio segment which may include the phoneme coarticulation with appropriately chosen window size. Nonetheless, in all these works, the temporal dependency in content (i.e., face) is largely left out and the coarticulation effect cannot be adequately modeled.

On the other hand, temporal-dependent methods such as [1] model the dynamic of audio features through recurrent neural network (RNN). The audio feature is used to represent the lip shape. By measuring the similarity between the given probe audio feature and the gallery audio feature set which are extracted from the source video set, they can find the best matched mouth region. The matched mouth sequence and the target video are re-timed and synthesized into the output video. Although the result seems very promising, it only works for the given person (Obama) which restricts the generalization capability. In addition, this method only models the lip and mouth region. The expression and head pose variation all depend on the source video which may generate inconsistent result with different audio as inputs.

Based on the analyses above, our proposed framework incorporates both image and audio in the recurrent unit to achieve temporal dependency in the generated video on both facial and lip movement, such that smooth transition across different video frames can be realized. In addition, we deploy a multi-task discriminator to improve the audio and lip shape consistency and photo-realism. Compared to previous approaches, no extra image deblurring procedures are needed in our framework. We have evaluated the performance of the proposed approach on several popular datasets. From the experiments, we have found that learning from the video dataset is more time consuming compared to the general image perception tasks, especially for the uncontrolled interview and news video dataset. On the other hand, we observe that these wild data usually present a biased phoneme distribution where some typical set of words appear more frequently. Repeatedly learning the same phoneme in the given deep learning framework then becomes unnecessary for training discriminative audio features. To reduce the training cost, we propose a sample selection approach to reducing

the size of training data by removing redundant samples without sacrificing performance. Our contributions are thus summarized as follows:

- We propose a novel conditional recurrent generation network to generate accurate lip sync and incorporate temporal dependency while maintaining smooth transition for both lip and facial movements.
- We deploy a multi-task discriminator to improve the lip sync accuracy and photo-realism.
- We develop a sample selection method which largely removes the highly redundant samples without sacrificing performance.

## 2 Related Work

In this section, we mainly review three related works, including speech face animation, conditional image generation, video prediction and generation.

### 2.1 Speech Face Animation

Speech face animation is a computer graphic problem that models and controls the facial features to synchronize lip motion with the audio. Traditional speech animation methods either use professional animators to manually produce the result or simply use the lip viseme gallery to synthesize speech animation. The former is time consuming and costly, while the latter generates low quality and less discriminative result. Since the lip motion is a complex and codependent facial action with the muscle, chin, tongue and etc, recent works apply neural network to achieve more accurate performance.

In recent years, some new developments have been reported. For example, [1] trained the lip model for only one person, i.e., President Barack Obama. The basic idea is to find the best matched mouth region image from his mouth gallery through audio features matching. And the final whole face image was not generated but synthesized by composing the mouth image with the target video. The trained model is difficult to adapt to other persons due to the large variation in mouth texture and content. [3] learned a mapping between raw audio and 3D meshes by an end-to-end network. In addition, an extra branch of emotional representation learning was needed to increase the photo-realism. Since this method aims to generate 3D mesh animation, it cannot capture the tongue, wrinkles, eyes, head motion which is required for image level face animation.

[2] proposed a conditional auto-encoder based network, where the audio feature and image identity feature were extracted by two convolutional encoder networks, respectively. The intuition is conditional image manipulation where by fixing the identity feature and changing the condition variables (i.e., the audio feature), the same face with different lip shape images can be generated. However, this work generates each single frame independently which breaks the temporal dependency between frames. Although the results demonstrate accurate lip shape and better generality, the result looks unreal with rigid lip motion and unchanged face expression, pose, etc.

[4] learned the mapping between audio and phoneme categories, then matched the best predefined lip region model according to the phoneme label. The final output was generated by re-targeting the lip region model with given input. The phoneme label is either manually provided by human or automatically generated by a speech recognition system. Manually providing phoneme is time consuming and cost inefficient which also limited the real-time application, while automatic phoneme labeling tends to be error-prone and restricts the performance.

## 2.2 Conditional Generation Adversarial Net

Generative adversarial network (GAN) [5] was first proposed in 2014 by Goodfellow which is able to generate photo-realistic images and has gained extraordinary popularity within recent two years. Compared with other generative models, such as variational autoencoder (VAE), GAN can generate much sharper and more photo-realistic images. Compared with the vanilla GAN, condition GANs can generate images under controllable factors rather than generating images from random noise. For example, Pix2pix [6] and CycleGAN [7] generated images with different color, style, and content conditioning on given reference images. CAAE [8] generated face with aging effect conditioning on different age labels. SRGAN [9] generated super-resolution images conditioning on low resolution images. [10] filled in the incomplete holes of an image conditioning on the surrounding pixels. Most aforementioned works conduct image generation or translation within the same modality (i.e., image modality). Few works conducted image generation between different modalities with large variations. For example, the text to image generation works [11][12] synthesized image content based on given text description. [9] predicted instrument images by providing the music audio played by some instruments.

## 2.3 Video Prediction and Generation

Video prediction has been widely studied in many works [13,14,15,16] which aims to predict the future frames conditioned on several previous frames. Different from video prediction, video generation directly generates frame sequences from noise. With the success of adversarial image generation network, a few works have attempted to generating videos through the adversarial training procedure. [17] decomposed video generation into motion dynamic and background content generation, where background image is generated using 2D convolution while the foreground motion which contains temporal information is modeled by 3D convolution. In this case, it is restricted to generate only fixed length videos. MoCoGAN [18] disentangled the video generation problem as content and motion generation. By fixing the content representation and changing the motion latent variables, the video can be generated with motion dynamic under the same content. Similarly, [19] decomposed the motion and content, and the future frame is predicted with fixed content and dynamic motion.

Audio to video generation is different from these two works since the audio information needs to be considered as condition and only one reference image

is provided which is difficult to hallucinate pixel values without capturing the flow change information between multiple frames. Rather than generating video from noise, the generated frames should have stable image content with accurate lip motion corresponding to the speech audio condition. In order to generate smooth video with flexible length, recurrent neural network is applied on the motion latent variable.

### 3 Proposed Method

In this section, we first overview the baseline method [2] which is the conditional auto-encoder based face generation network. We then describe the proposed method where both image and audio representations are encoded by gated recurrent unit to incorporate the temporal-dependent information. The proposed method is trained using an adversarial training scheme to avoid blur result. Multi-task discriminator is applied here to both improve the lip sync accuracy as well as photo-realism. We envision the computational complexity of training induced by large amount of training samples, and propose a sample selection method to speed up the training time without sacrificing the performance.

#### 3.1 Conditional Face Generation Network Baseline

Since the proposed work is closely related to the Speech2Vid [2] method which is a conditional autoencoder based audio-to-video generation network, we use it as a baseline and first describe its framework in this section. In Speech2Vid, audio segments are cropped from the entire audio clip using sliding window. Frames that have the corresponding lip shapes are extracted from the audio segments. Only one frame is used as ground truth to each audio segment as shown in Fig. 1. In order to control different lip shapes and audio signals, both the image feature and audio feature are encoded through convolution neural network (i.e., image encoder  $E_I$ , and audio encoder  $E_A$ ) and concatenated together. The concatenated feature is later decoded to generate the target image with desired lip shape while preserving the same identity using the decoder network  $G$ . U-Net [20] is also adopted to largely preserve the identity, especially for unseen faces. Since the reconstruction loss as shown in Eq. 1 is the only objective function to guide the lip shape, it addresses blur results especially around the mouth region using an extra deblur network,

$$\mathcal{L}_{rec} = \left\| I_t - \tilde{I}_t \right\|_1, \quad (1)$$

where  $\tilde{I}_t = G(z^I, z^A)$  and  $I_t$  are the generated and ground truth video frames, respectively;  $z^I = E_I(I_0)$  represents the image feature of the given reference image  $I_0$ , and  $z^t = E_A(A_t)$  represents the audio feature of the audio segment. It is important to point out that in Speech2Vid, since features are extracted from individual audio segments using the sliding window, temporal dependency is not realized, leading to unreal visual quality and unsmooth transition between frames.

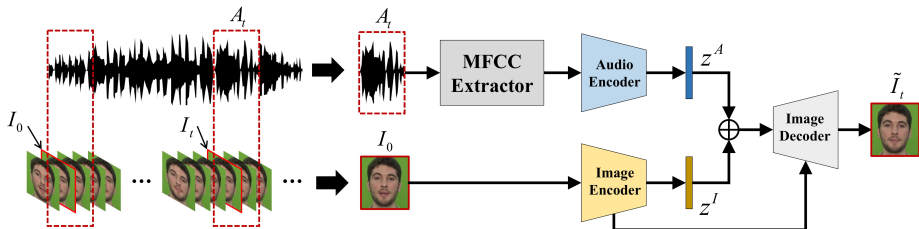


Fig. 1: Conditional autoencoder based audio to video generation network structure [2]. Mel-Frequency Cepstral Coefficients (MFCC) features are extracted and fed into a convolutional encoder network. Image identity information is also encoded by convolutional network. The audio feature  $z^A$  and image feature  $z^I$  are 1D vector extracted from fully connected layers. The final image is reconstructed by an image decoder/generator.

### 3.2 Conditional Recurrent Adversarial Network

We improve the Speech2vid [2] framework by applying gated recurrent unit (GRU) on both image and audio features. It is worth mentioning that although applying the recurrent unit on audio feature alone can improve the lip shape smoothness, for datasets in the wild, due to the large variation of pose and motion, the generated video tends to exhibit jitter effect where transition between frames is not smooth. Therefore, it is essential to apply GRU on both features.

**Audio Feature Discussion** In recent audio to video works, different types of audio information have been employed, including, for example, the raw audio [3], the Mel-Frequency Cepstral Coefficients (MFCC) features of audio [1][2], and the Log-amplitude of Mel-Spectrum (LMS) [21]. We choose the MFCC feature due to its effectiveness in speech recognition, good linear separation between phonemes, and readiness to work with RNN models. In addition, for fair comparison with the baseline method, we use the same protocol as [2], where each audio segment corresponds to 350ms information. Each MFCC feature is extracted from a length of 20ms audio segment with overlap of 10ms. We remove the first coefficient from original MFCC vector, eventually yielding a  $35 \times 12$  MFCC features for each audio segment.

**Conditional Recurrent Video Generation** The proposed conditional recurrent video generation network is shown in Fig. 2. A series of audio feature variables are denoted as  $z^A = [z_0^A, z_1^A, \dots, z_k^A, \dots, z_t^A]$  and the image feature  $z^I$  is concatenated with  $z^A$  to generate a hybrid feature where both the face and audio information are incorporated. At each time step,  $k$ , this hybrid feature, denoted as  $\tilde{z}_k = \{z_k^A, z^I\}$ ,  $\tilde{z}_k \in \tilde{Z}$ , serves as the input to the recurrent unit. Let  $R_E$  denote the recurrent encoder network, then the output  $R_E(\tilde{Z})$ , will be used by the image decoder to generate frames in the video clip  $\tilde{I} = [\tilde{I}_0, \tilde{I}_1, \dots, \tilde{I}_t]$ .

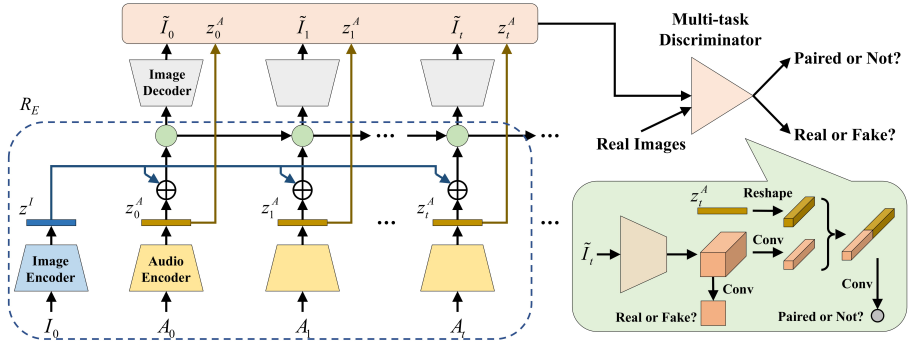


Fig. 2: The proposed conditional recurrent adversarial video generation network structure.

The motivation behind using the hybrid feature is that the current lip movement is also affected by previous lip shapes, and the recurrent neural network can better represent the video dynamics by mapping independent features to a sequence of correlated features. Intuitively, we can apply the recurrent unit on audio features alone to build the temporal dependency and achieve smooth lip movement. However, due to the variation of input faces, it cannot preserve the image smoothness nor the smooth transition. Applying recurrent unit on the hybrid code of image and audio features leads to a smooth change of content and largely improved video quality.

**Multi-task Discriminator** In traditional GAN, the discriminator is designed to differentiate real images from fake ones (i.e., generated image) to improve the photo-realism. We refer to this type of discriminator as “image-aware discriminator”. In some conditional GAN works, the discriminator also aims to distinguish whether the two inputs are real pair (i.e., the image under the corresponding condition) or not. We refer to this type of discriminator as “matching-aware discriminator”, following the work of [11]. In this work, we adopt both image-aware discriminator and matching-aware discriminator to improve the image quality and also the lip shape sync accuracy. For image-aware discriminator, patch discriminator as mentioned in Pix2pix [6] is adopted to keep more details around the mouth region. The real image is the ground truth face corresponding to an audio segment and the fake image is the generated face conditioned on the audio input. The output is a grid of binary map which indicates the real or fake with respect to local image regions. For matching-aware discriminator, the real sample is the real face image and its corresponding audio feature, and the fake sample contains two cases, one is the generated face image under given audio condition, another is the real face with mismatch audio condition. The mismatch audio condition is generated by shuffling or shifting the audio feature from the ground truth face images. The output is either 1 or 0 which indicates whether it is a matched pair or not. The upper layer of these two discriminators are shared

for these two tasks. The loss functions on both the discriminator  $D$  and image generator/decoder  $G$  are written in Eqs. 2 and 3, respectively.

$$\mathcal{L}_G = \underbrace{\mathbb{E}_{I \sim \mathbb{P}_r} [\log(1 - D(I))]}_{\text{Unconditioned}} + \underbrace{\mathbb{E}_{\tilde{I} \sim \mathbb{P}_g} [\log(1 - D(\tilde{I}, z_I))]}_{\text{Conditioned}} \quad (2)$$

$$\mathcal{L}_D = \underbrace{-\mathbb{E}_{I \sim \mathbb{P}_r} [\log D(I)] - \mathbb{E}_{\tilde{I} \sim \mathbb{P}_g} [\log(1 - D(\tilde{I}))]}_{\text{Unconditioned}} - \quad (3)$$

$$\underbrace{\mathbb{E}_{I \sim \mathbb{P}_r} [\log(1 - D(I, z_I))] - \mathbb{E}_{I \sim \mathbb{P}_r} [\log(1 - D(I, \hat{z}_I))] - \mathbb{E}_{\tilde{I} \sim \mathbb{P}_g} [\log(1 - D(\tilde{I}, z_I))]}_{\text{conditioned}}$$

where  $I$  and  $\tilde{I}$  are the real and generated image, respectively, under the matched condition; and  $z_I$  and  $\hat{z}_I$  are the mismatched condition with real image  $I$ .

To further improve the image quality, the perceptual loss [22] based on VGG Face Net [23] is adopted as in Eq. 4,

$$\mathcal{L}_{per} = \sum_{i=1}^C \left\| \phi_i(I) - \phi_i(\tilde{I}) \right\|, \quad (4)$$

where  $\phi_i$  denotes the  $i$ -th feature layer, and the accumulated difference between  $C$  layers is calculated.

The final objective function is

$$\min_{G, E_A, E_I, R_E} \max_D \mathcal{F}(G, E_A, E_I, R_E, D), \quad (5)$$

where  $\mathcal{F}(G, E_A, E_I, R_E, D) = L_{rec} + \gamma L_{per} + \lambda L_G + \lambda L_D$ .

### 3.3 Sample Selection

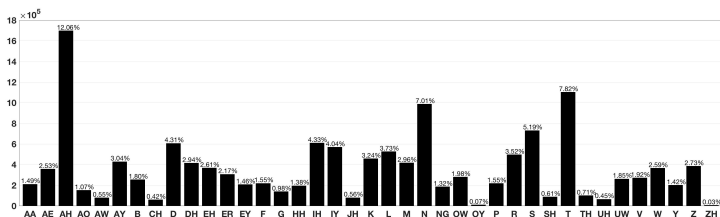
Most recent audio to video works capitalize on the large amount of talking face dataset from website, for example, the news, interview, etc. Although learning from large dataset which contains rich information can achieve good generalization and discriminative capability, it also consumes the training time. For example, [1] collected around 300 videos from Obama’s weekly addresses. The Vox-Celeb dataset [24] contains 1,251 celebrities, for each identity there are around 10 video sequences, and each video is segmented into different clips to guarantee that only one single person’s face appears in the video. Training on such large dataset is inefficient and quite time consuming, especially for video generation tasks.

Phoneme is the smallest detectable unit of a language and is produced by a combination of the movement of lips, teeth, and tongues of the speaker. We first exploit the phoneme distribution of the original dataset by extracting all the phonemes from the videos. In order to obtain the phoneme histogram for each audio sample, we use the “you-get” [25] tool to fetch the valid English subtitles

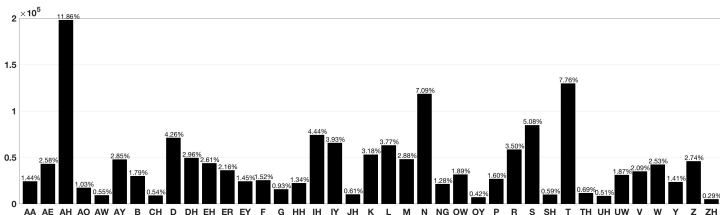


based on the YouTube ID provided by VoxCeleb. Then audio and subtitle are aligned by the Penn Phonetics Lab Forced Aligner (P2FA) [26] tools. This is followed by phonemes being extracted by the CMU Lexicon Tool [27] which defines 39 phoneme categories. Finally we select more than 15,114 videos which have valid English subtitle files. The overall phoneme histogram is shown in Fig. 3. It is easy to observe that the phoneme “ZH” only appears 4,800 times while “AH” appears 11,010,000 times.

Based on the above analyses, we propose a sample selection method to drastically reduce the number of training samples taking advantage of the biased histogram of different phonemes without affecting the general distribution of the phoneme. The details about our sample selection algorithm are described in the supplement.



(a)



(b)

Fig. 3: The phoneme histogram before (a) and after (b) sample selection.

## 4 Experiments and Results

We evaluate the effectiveness of the proposed method on two popular datasets. We mainly use the quality of the generated lip shape and the smoothness of the video to evaluate the performance. The quality of the generated lip shape is measured by the synchronization accuracy of the lip shape movement. The smoothness measures if there is any unreasonable pixel changes across the generated frames. Both quantitative and qualitative evaluations are conducted to

demonstrate the generalization capacity and generated video quality of the proposed approach. Considering the challenges of evaluating the generated video quality and lip shape accuracy, we also conduct two user studies to perform perceptual evaluation.

#### 4.1 Datasets and Compared Methods

**TCD** [28] dataset is initially built for speech recognition purpose where the sentences read by human contain rich phoneme categories. The entire dataset contains audio and video footages of 62 speakers. In total, there are 6,913 phonetically rich sentences. All the videos are collected under a well-controlled environment. We follow the same splitting policy in the original paper for building the training and testing set.

**VoxCeleb** [24] dataset contains more than 20,000 videos from 1,251 celebrities. In our experimental setting, we select 9,514 training samples from 1,129 identities which contain valid English subtitles for better understanding of the dataset. The test samples are selected from the rest. Different from the TCD dataset, VoxCeleb dataset contains large variations in talking speed, accent, etc. The face images are also with different poses, illuminations, and occlusions. Pre-processing is applied to normalize all audio to 16KHz. Faces with extreme pose variations are filtered out based on the landmark information.

**Compared Methods** We compare the proposed approach with two other approaches. The first is the conditional autoencoder network [2], and the other is RNN on audio features with different losses. We denote the conditional autoencoder based baseline <sup>3</sup> as “CAE”, and the proposed method as “RAE<sub>IA</sub>-PG” where temporal cues from both image (I) and audio (A) representations are captured via RNN. Our proposed framework also integrates the perceptual loss (P) and GAN (G) loss to further improve the image quality. Similarly, if only using RNN to model the audio feature, we denote it as “RAE<sub>A</sub>”.

#### 4.2 Implementation Details

**Training scheme** In this work, we adopt incremental training scheme to build our deep model. The perceptual loss and adversarial loss are added when “CAE” is trained to be stable. The weights for perceptual loss and adversarial loss are set to be 1e-4, 1e-3, respectively. In order to preserve the identity especially for unseen people which are not included in the training data, Chung et al. [2] suggests using U-Net structure to keep the face identity. In this work, the authors also use multiple frames as input to further improve the image quality. However, this approach will increase the training time and generate unrealistic results where only the lip is moving while other facial parts remain still across the entire video sequence. In our experimental setting, only one frame is used as the reference image. If faces with extreme pose are removed, we will take the longest consecutive sequence within this video for training the RNN network.

<sup>3</sup> We reimplemented the whole framework, for fair comparison, all network structure are the same as previous structure.

**Network architectures** The audio, image encoder, and image decoder networks are all implemented using convolution and deconvolution models. More details can be found in the supplementary material. We apply GRU with orthogonalized initialization for our recurrent network. ADAM [29] ( $\alpha = 0.0002$ ,  $\beta = 0.5$ ) optimizer is adopted. We have exploited two different training schemes, i.e., training RNN from scratch and training on pre-trained CAE network. We discover that the latter converges much faster. Hence we first train CAE with 50 epochs, then perceptual loss and adversarial loss are added to train for another 30 epochs. In the end, RAE is fine-tuned on the pretrained CAE model for another 50 epochs. In the whole framework, we set the image size as  $112 \times 112$ . The length of training image sequence is 70.

### 4.3 Qualitative Comparison

**Generalization Analysis** To demonstrate the superior generalization capability of the proposed approach, we evaluate the performance of the proposed pipeline on unseen videos and unseen faces. As illustrated in Fig. 4 which gives generated results for different input identities using the same audio. We can observe that the proposed method generates consistent lip shape movement across different identities. The generalization accuracy can also be measured by comparing the generated results with the ground truth images shown on the top. Similarly, the result on Voxceleb dataset is shown at the bottom of Fig. 4. Both results demonstrate that the proposed method works well in controlled as well as uncontrolled environments.

**Comparison with different methods** To evaluate the performance of our generation framework in improving the smoothness of lip and facial motion, especially the benefit from capturing the temporal information on both image and audio features, we compare with another two methods using the same testing samples from TCD and Voxceleb dataset, respectively. For ablation analysis, adversarial loss and perceptual loss are excluded for all these three compared approaches.

As shown in Fig. 5<sup>4</sup>, in order to measure the stability of generated image frames, the optical flow between each two continuous frames is calculated.  $(u, v) = \text{opticalflow}(I_1, I_2)$ . We first define the movement intensity for each pixel as  $u^2 + v^2$ . The average movement intensity map is generated as demonstrated in Fig. 5 (c). The brighter color represents larger pixel movement. By comparing the movement intensity map which is calculated on the entire sequence, rather than the four frames shown, we observe that RAE<sub>IA</sub> generates more smooth videos, and most movements are around the mouth region. Comparing CAE with RAE<sub>A</sub> and RAE<sub>IA</sub>, CAE may generate unclear and unsmooth lip movements as pointed out by the red arrow. Even RAE<sub>A</sub> improves the smoothness of lip movement, it cannot guarantee the smoothness in facial movement between

<sup>4</sup> Better to see results in video on project page.



Fig. 4: The generated image sequences by providing an identity image shown in the red box on the left and an audio segment. By changing the identity while fixing the audio input, the generated result demonstrates the consistent lip shape change. And the accuracy can be found by comparing with the ground truth image as shown in the black box on the top. Top: the result from TCD set. Bottom: the result from VoxCeleb dataset. It is interesting to see that the 2nd and 3rd frames (highlighted by red dashed box) do not present smooth transition from the 1st frame, however, the proposed method is able to reject the anomaly by considering the information from the previous frame, i.e., temporal dependency.

frames. From the example listed at the bottom of Fig. 5, we observe that the face shapes are not consistent between frames.

#### 4.4 Quantitative Evaluation

**Evaluation on Image Generation Performance** The inception score with different loss functions on both TCD and VoxCeleb datasets are shown in Table 1. From Table 2, we could better visualize the effects of different loss functions. With both perceptual loss and adversarial loss, more detailed textures are kept, e.g., the teeth.

**User Study** We conduct two user studies to quantitatively compare performance using different methods. We mainly compare the CAE network [2], RAE with perceptual loss and adversarial loss/GAN loss, denoted as “CAE-PG”, and

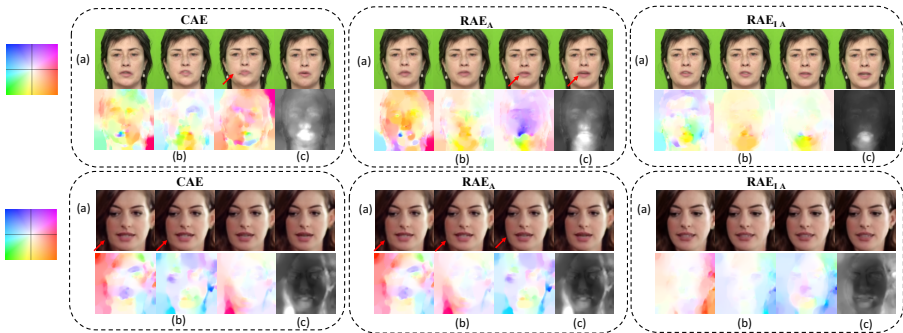


Fig. 5: We randomly select two test samples from TCD and Voxceleb datasets to demonstrate the difference between CAE,  $RAE_A$  and  $RAE_{IA}$ . (a) Generated frame sequence selected from the entire sequence for better visualization purpose. The corresponding optical flow map between two frames are shown in (b). The movement intensity map is calculated on the entire sequence as shown in (c). The inconsistent and abnormal changes are pointed out by red arrows. The motion map is shown on the left for better understanding of the movement direction and intensity.

“ $RAE_A$ -PG” and the proposed “ $RAE_{IA}$ -PG”. We choose Amazon Mechanical Turk (AMT) as the user study platform for evaluation. All the workers are specified to be either “UK” or “USA”. The first user study lets the workers choose their preferred video result according to video quality, video smoothness and photo-realism. We generate 60 test samples for TCD and VoxCeleb dataset, respectively. For each test sample, results generated by different methods are provided to workers, and they are asked to choose which one is better. Each question is answered by 10 different workers. The result is demonstrated in Table 3.

Dataset	$L_{rec}$	$+L_{pec}$	$+L_{pec} + L_{adv}$
TCD	$1.51 \pm 0.12$	$1.61 \pm 0.10$	$1.83 \pm 0.07$
Vox-Celeb	$1.52 \pm 0.26$	$1.54 \pm 0.23$	$1.58 \pm 0.19$

Table 1: Comparison between different losses on inception score for TCD and VoxCeleb Dataset on RNN based network.



Table 2: Qualitative result after adding different losses. Left: Only the reconstruction loss is used. Middle: Reconstruction loss with perceptual loss. Right: Reconstruction loss with perceptual loss and adversarial loss

Table 3: User preference score on the quality of generated videos.

Dataset	CAE	CAE-PG	RAE <sub>A</sub> -PG	RAE <sub>I,A</sub> -PG
TCD	12%	21%	28%	39%
Voxceleb	15%	19%	30%	36%

The second user study aims to evaluate the lip sync accuracy. We define four accuracy levels as shown in Table 4. For example,  $> 80$  means that more than 80% of the entire frames are with accurate lip synchronization. The testing samples are the same as the first user study.

Table 4: The evaluation of lip sync accuracy on TCD (left) and VoxCeleb dataset(right).

Method	$> 80$	$50 - 80$	$30 - 50$	$< 30$	$> 80$	$50 - 80$	$30 - 50$	$< 30$
CAE	27%	22%	35%	16%	15%	32%	33%	20%
CAE-PG	37%	41%	16%	6%	18%	34%	30%	18%
RAE <sub>A</sub> -PG	40%	34%	19%	7%	21%	34%	19%	16%
RAE <sub>I,A</sub> -PG	45%	32%	18%	5%	29%	47%	13%	11%

From these two user studies, we discover that the proposed method achieves much better result on TCD dataset as compared to VoxCeleb dataset. The main reason is that the VoxCeleb dataset is recorded in uncontrolled environment which contains lots of noise, large variations of head poses and background changes.

## 5 Conclusion

We presented a synchronized audio to talking video generation framework. Our framework mainly utilizes the recurrent adversarial network to model the temporal correlation of audio features and facial image features at the same time. This has shown to greatly improve the photo-realism as well as smoothness in both lip and facial movement for the generated video data. We demonstrated the superiority on both controlled and uncontrolled datasets as compared to state-of-the-art approaches. We also proposed a sample selection method which largely reduces the training size by removing highly frequent samples without sacrificing performance.

The current audio encoder network still needs the off-the-shelf audio extractor which may limit the performance of the end-to-end training. More efforts need to be put in on the high resolution video generation task.

## References

1. Suwajanakorn, S., Seitz, S.M., Kemelmacher-Shlizerman, I.: Synthesizing obama: learning lip sync from audio. *ACM Transactions on Graphics (TOG)* **36**(4) (2017) 95
2. Chung, J.S., Jamaludin, A., Zisserman, A.: You said that? *British Machine Vision Conference (BMVC)* (2017)
3. Karras, T., Aila, T., Laine, S., Herva, A., Lehtinen, J.: Audio-driven facial animation by joint end-to-end learning of pose and emotion. *ACM Transactions on Graphics (TOG)* **36**(4) (2017) 94
4. Taylor, S., Kim, T., Yue, Y., Mahler, M., Krahe, J., Rodriguez, A.G., Hodgins, J., Matthews, I.: A deep learning approach for generalized speech animation. *ACM Transactions on Graphics (TOG)* **36**(4) (2017) 93
5. Goodfellow, I., Pouget-Abadie, J., Mirza, M., Xu, B., Warde-Farley, D., Ozair, S., Courville, A., Bengio, Y.: Generative adversarial nets. In: *Advances in neural information processing systems*. (2014) 2672–2680
6. Isola, P., Zhu, J.Y., Zhou, T., Efros, A.A.: Image-to-image translation with conditional adversarial networks. *CVPR* (2017)
7. Zhu, J.Y., Park, T., Isola, P., Efros, A.A.: Unpaired image-to-image translation using cycle-consistent adversarial networks. In: *Computer Vision (ICCV), 2017 IEEE International Conference on*. (2017)
8. Zhang, Z., Song, Y., Qi, H.: Age progression/regression by conditional adversarial autoencoder. In: *IEEE Conference on Computer Vision and Pattern Recognition (CVPR)*. (2017)
9. Ledig, C., Theis, L., Huszár, F., Caballero, J., Cunningham, A., Acosta, A., Aitken, A., Tejani, A., Totz, J., Wang, Z., et al.: Photo-realistic single image super-resolution using a generative adversarial network. *CVPR* (2017)
10. Pathak, D., Krahenbuhl, P., Donahue, J., Darrell, T., Efros, A.A.: Context encoders: Feature learning by inpainting. In: *Proceedings of the IEEE Conference on Computer Vision and Pattern Recognition*. (2016) 2536–2544
11. Reed, S., Akata, Z., Yan, X., Logeswaran, L., Schiele, B., Lee, H.: Generative adversarial text to image synthesis. *ICML* (2016)
12. Zhang, H., Xu, T., Li, H., Zhang, S., Huang, X., Wang, X., Metaxas, D.: Stackgan: Text to photo-realistic image synthesis with stacked generative adversarial networks. In: *IEEE Int. Conf. Comput. Vision (ICCV)*. (2017) 5907–5915
13. Mathieu, M., Couprie, C., LeCun, Y.: Deep multi-scale video prediction beyond mean square error. *arXiv preprint arXiv:1511.05440* (2015)
14. Oh, J., Guo, X., Lee, H., Lewis, R.L., Singh, S.: Action-conditional video prediction using deep networks in atari games. In: *Advances in Neural Information Processing Systems*. (2015) 2863–2871
15. Srivastava, N., Mansimov, E., Salakhudinov, R.: Unsupervised learning of video representations using lstms. In: *International conference on machine learning*. (2015) 843–852
16. Liang, X., Lee, L., Dai, W., Xing, E.P.: Dual motion gan for future-flow embedded video prediction. *arXiv preprint* (2017)
17. Vondrick, C., Pirsiaavash, H., Torralba, A.: Generating videos with scene dynamics. In: *Advances In Neural Information Processing Systems*. (2016) 613–621
18. Tulyakov, S., Liu, M.Y., Yang, X., Kautz, J.: Mocogan: Decomposing motion and content for video generation. *arXiv preprint arXiv:1707.04993* (2017)

19. Villegas, R., Yang, J., Hong, S., Lin, X., Lee, H.: Decomposing motion and content for natural video sequence prediction. arXiv preprint arXiv:1706.08033 (2017)
20. Ronneberger, O., Fischer, P., Brox, T.: U-net: Convolutional networks for biomedical image segmentation. In: International Conference on Medical image computing and computer-assisted intervention, Springer (2015) 234–241
21. Chen, L., Srivastava, S., Duan, Z., Xu, C.: Deep cross-modal audio-visual generation. In: Proceedings of the on Thematic Workshops of ACM Multimedia 2017, ACM (2017) 349–357
22. Johnson, J., Alahi, A., Fei-Fei, L.: Perceptual losses for real-time style transfer and super-resolution. In: European Conference on Computer Vision, Springer (2016) 694–711
23. Parkhi, O.M., Vedaldi, A., Zisserman, A., et al.: Deep face recognition. In: BMVC. Volume 1. (2015) 6
24. Nagrani, A., Chung, J.S., Zisserman, A.: Voxceleb: a large-scale speaker identification dataset. arXiv preprint arXiv:1706.08612 (2017)
25. You-Get Tools: You-get tools. <https://github.com/soimort/you-get> [Online].
26. Penn Phonetics Lab: Penn Phonetics Lab Forced Align Tools. <https://github.com/ucbvislab/p2fa-vislab> [Online].
27. CMU Lextool Tools: Cmu lextool tools. <http://www.speech.cs.cmu.edu/tools/lextool.html> [Online].
28. Harte, N., Gillen, E.: Tcd-timit: An audio-visual corpus of continuous speech. *IEEE Transactions on Multimedia* **17**(5) (2015) 603–615
29. Kingma, D.P., Ba, J.: Adam: A method for stochastic optimization. arXiv preprint arXiv:1412.6980 (2014)



## Appendix

### Network Structure

The network structures of the audio encoder  $E_A$ , image encoder  $E_I$ , image decoder  $G$ , and multi-task discriminator  $D$  are shown in Tables 1-4, respectively. Unless otherwise specified, the kernel size, stride step and padding follow the default setting.

Table 5: Network structure of the audio encoder  $E_A$ . In this experiment setting, the default strides (S) is (1, 1), default kernel (K) size is 3 and the default padding (P) method is “SAME”.

#	Layer name(s)	Output size
0	Input	$12 \times 35 \times 1$
1	Conv, BN, ReLU	$12 \times 35 \times 64$
2	Conv, BN, ReLU	$12 \times 35 \times 128$
3	Maxpool, S=(1, 2)	$12 \times 18 \times 128$
4	Conv, BN, ReLU	$12 \times 18 \times 256$
5	Conv, BN, ReLU	$12 \times 18 \times 256$
6	Conv, BN, ReLU	$12 \times 18 \times 512$
7	Maxpool, S=(2, 2)	$6 \times 9 \times 512$
8	FC, BN, ReLU	512
Output $z^A$	FC	256

Table 6: Network structure of the image encoder  $E_I$ . The default strides (S) setting is (2, 2), the default kernel (K) size is 5, and the default padding (P) method is “SAME”.  $c$  is the number of input images.

#	Layer name(s)	Output size
0	Inputs	$112 \times 112 \times 3c$
1	Conv, BN, ReLU	$56 \times 56 \times 64$
2	Conv, BN, ReLU	$28 \times 28 \times 128$
3	Conv, BN, ReLU	$14 \times 14 \times 256$
4	Conv, BN, ReLU	$7 \times 7 \times 512$
5	FC, BN, ReLU	512
Output $z^I$	FC	256

### Sample Selection

Learning from large datasets which contain rich information could achieve good generative and discriminative capability. On the other hand, it is also very time-consuming to train on large datasets. Sample selection aims to select video clips,

Table 7: Network structure of the image decoder  $G$ . The default strides (S) setting is (2, 2), the default kernel (K) size is 5, and the default padding (P) method is “SAME”.

#	Layer name(s)	Output size
0	Inputs: $z^A$ and $z^I$	(256 + 256)
1	FC, BN, ReLU	25088
2	Deconv, BN, ReLU	$14 \times 14 \times (256 + 256)$
3	Deconv, BN, ReLU	$28 \times 28 \times (128 + 128)$
4	Deconv, BN, ReLU	$56 \times 56 \times (64 + 64)$
5	Deconv, BN, ReLU	$112 \times 112 \times 32$
Output	Deconv, Tanh	$112 \times 112 \times 3$

Table 8: Network structure of the multi-task discriminator  $D$ . The default strides (S) setting is (2, 2), the default kernel (K) size is 4, and the default padding (P) method is “SAME”. Output1 and output2 are “image-aware”, “matching-aware” results, respectively.

#	Layer name(s)	Output size
0	Inputs	$112 \times 112 \times c$ and $z^A$
1	Conv, BN, ReLU	$56 \times 56 \times 16$
2	Conv, BN, ReLU	$28 \times 28 \times 32$
3	Conv, BN, ReLU	$14 \times 14 \times 64$
4	Conv, BN, ReLU	$7 \times 7 \times 128$
Output1	Conv	$7 \times 7 \times 1$
5	Conv, BN, ReLU	$4 \times 4 \times (256 + 256)$
6	Conv, BN, ReLU, K=1, S=(1,1)	$4 \times 4 \times 128$
Output2	Conv, P=Valid	$1 \times 1 \times 1$

taking advantage of the phoneme distribution information, where phonemes with lower occurrence rate are kept and those with higher occurrence rate (i.e., more repeated and redundant phonemes) are randomly removed. The details of sample selection is shown in Algorithm 1. To preserve those more important phonemes with lower occurrence rate in sample selection, the video clips are first ranked according to their individual phoneme distribution, where the lower the occurrence rate, the higher the rank of the phoneme. Then, samples are selected based on the rank. We randomly select  $n$  sample where  $n$  is in range of  $n_{min}$ , and  $n_{max}$ . In the experiment,  $n_{min}$  is set to be 5,000 and  $n_{max}$  to be 15,114. We repeat this selection  $k$  times where  $k$  is set to be 50. The best result is the one with shortest distance to uniform distribution,  $\mathbb{U}$ .

---

**Algorithm 1:** Sample Selection Algorithm
 

---

**Input** : A list of video clips  $F_N$ .

**Output** : A list of selected video clips  $F_n$ .

**Initialization:** The overall phoneme distribution  $\mathbb{P}_{ph}$ .

The maximum and minimum length of  $F_n$ ,  $n_{max}$  and  $n_{min}$ .

The initial selection criterion  $\delta$ , and iteration times  $k$ .

```

1  $R_{ph} \leftarrow \text{sort}(\mathbb{P}_{ph}, \text{ascending})$ 
2  $F_N \leftarrow \text{sort}(F_N, R_{ph})$ 
3 for 1 to  $k$  do
4   Randomly sample  $n \sim \mathbb{U}(n_{min}, n_{max})$ .
5   Calculate phoneme distribution of the top  $n$  video clips,  $\mathbb{P}_{ph}^n$ 
6   if  $\text{dist}(\mathbb{P}_{ph}^n, \mathbb{U}) < \delta$  then
7      $\delta = \text{dist}(\mathbb{P}_{ph}^n, \mathbb{U})$ 
8      $F_n \leftarrow$  top  $n$  of  $F_N$ 
9   end
10 end

```

---